

Cite this: *J. Mater. Chem. B*, 2023, **11**, 5786

Biocompatible cationic polypeptoids with antibacterial selectivity depending on hydrophobic carbon chain length†

Xiran Shen,^{ab} Yu Rao,^b Di Liu,^a Jinghong Wang,^{cd} Xiaomeng Niu,^b Yichen Wang,^b Wentao Chen,^b Fan Liu,^b Li Guo^{id *e} and Hong Chen^{id b}

The overuse of antibiotics has triggered a new infection crisis and natural antimicrobial peptides (AMPs) have been extensively studied as an alternative to fight microorganisms. Polypeptoids, or polypeptide-biomimetics, offer similar properties to polypeptides and a highly tunable structure that has been synthesized by various methods such as ring opening polymerization (ROP) using *N*-carboxyanhydride monomers. Simultaneous high antibacterial activity and biocompatibility of a structure by efficient synthesis is desired in the application of those materials. Herein, a series of cationic polypeptoids (PNBs) with variable side chain lengths was obtained by introducing positive charges to the main chain in one step and preserving the backbone structure, namely polypeptoids (PNBM, PNBE, PNBB) with different end groups (methyl (M), ethyl (E), butyl (B)). To address the issue of infection in interventional biomedical implants, we report cost-effective modified polyurethane (PU) films (PU-PNBM, PU-PNBE, PU-PNBB) as physical-biological synergistic antibacterial surfaces that overcome problems such as steric hindrance and the solubility of the materials. Antibacterial selectivity was achieved by regulating the different side chain lengths. When methyl and ethyl were used as hydrophobic side chains, they can only selectively kill Gram-positive *Staphylococcus aureus*. PNBB, the most hydrophobic and with a butyl side chain can kill both Gram-negative *Escherichia coli* and Gram-positive *Staphylococcus aureus* and inhibit the growth of bacterial biofilms. Effective in both solution and modified substrate, its biocompatibility is not compromised while the antibacterial properties are substantially improved. Furthermore, PU-PNBB films demonstrated their potential *in vivo* antimicrobial efficiency in a model of *S. aureus* infection established on mouse skin. The synthesis route and the surface modification strategies are convenient, providing a solution to the problem of poor biocompatibility in antimicrobial surface applications and a strategy for the use of peptide polymers for targeted therapy after specific infections in the biomedical field.

Received 25th March 2023,
Accepted 22nd May 2023

DOI: 10.1039/d3tb00643c

rsc.li/materials-b

1. Introduction

Antimicrobial peptides (AMPs) have been widely recognized as a promising solution against multidrug-resistant bacteria.¹ Unlike conventional antibiotics, AMPs can interact with specific cells

and disrupt the morphology of bacteria through electrostatic interactions.² This antibacterial mechanism keeps bacteria from becoming resistant to AMPs. However, natural AMPs are limited in their clinical use,^{3–5} mainly due to their high toxicity to mammalian cells.⁶ Moreover, low synthesis efficiency and limited structural diversity restrict AMPs' application. It is of great importance to develop alternatives with excellent biocompatibility and structural flexibility by an improved synthesis method.

Artificially synthesized AMPs display great application potential and receive a lot attention as effective antimicrobial agents.^{7–9} These polymeric antibacterial agents, such as polyacrylates,¹⁰ polynorbornenes,¹¹ and polypeptides,¹² offer significant improvements over natural AMPs, including superior stability, ease of synthesis, and low cost.^{13–17} Polypeptoids with a degradable backbone,¹⁸ also known as *N*-substituted glycines, represent one of the most important peptide analogues and show great potential in various biomedical applications.¹⁹ The highly

^a Research School of Polymeric Materials, School of Material Science & Engineering, Jiangsu University, Zhenjiang, 202113, P. R. China. E-mail: liguo@ujs.edu.cn

^b State and Local Joint Engineering Laboratory for Novel Functional Polymeric Materials, College of Chemistry, Chemical Engineering and Materials Science, Soochow University, Suzhou 215123, P. R. China

^c Jiangsu Biosurf Biotech Co., Ltd, Suzhou 215123, P. R. China

^d The SIP Biointerface Engineering Research Institute, Suzhou 215123, P. R. China

^e Jiangsu Key Laboratory of Neuropsychiatric Diseases, College of Pharmaceutical Sciences, Soochow University, Suzhou 215123, P. R. China.
E-mail: liufan@suda.edu.cn

† Electronic supplementary information (ESI) available. See DOI: <https://doi.org/10.1039/d3tb00643c>

tunable structure of polypeptoids means that they retain the backbone structure of the polypeptide and lose the chiral center and hydrogen bond, thus providing better biocompatibility and protein bioactivity.^{20–27} The widely chosen solid-phase synthesis methods^{28,29} can produce precisely sequenced peptides, but the drawbacks include low yield and short peptide chains. Ring-opening polymerization (ROP) of *N*-carboxyanhydrides (NCAs) has been proposed as a versatile method for the synthesis of antibacterial polypeptides/polypeptoids.^{30–32} It provides an efficient and convenient approach for peptide polymer synthetic targets with complex macromolecular structures, such as polymeric nanoparticles of various conformations.^{33,34} The antibacterial mechanisms of AMPs are currently classified into three main types: membrane destructive, nondestructive membrane disturbance, and intracellular targeting mechanisms.³⁵ Their tunable antibacterial properties have been extensively studied through the synthesis of peptides/peptoids with both cationic and hydrophobic fragments. In many studies, the cationic groups and hydrophobic fragments are not in the same center, which greatly increases the difficulty of polymerization. The complexity of the molecular backbone structure also affects the action of the cationic groups. This synergistic mechanism makes it difficult to obtain polymers with excellent biocompatibility.^{36–38} The reduction of structural complexity is also desired for structural design and engineering.³⁹ To this end, in our work, the cationic sites and hydrophobic fragments of our antibacterial polymers were designed to be in the “same center”.

Recently, many researchers have developed a series of novel antibacterial agents by exploiting the cationic and amphiphilic synergistic mechanism of AMP in the design and chemical synthesis of antimicrobial polymers. Those polymers have easily post-modified structures, improved cytocompatibility, and low immunogenicity. For example, Sun's group⁴⁰ developed sulfonium-containing polypeptoids and explored the effects of the cationic and amphiphilic properties on their antimicrobial and hemolytic activities. The antibacterial activity decreased at low levels of hydrophobic units, while the hemolytic activity increased at high levels of hydrophobic units. Liu's group⁴¹ reported a simple and economical thermoplastic polyurethane (TPU) surface-modified peptide polymer with broad-spectrum antibacterial properties and effective *in vitro* thixotropic ability which exhibited good biocompatibility and showed no hemolysis or cytotoxicity. These studies suggest that the key to modulating the antibacterial activity and cytocompatibility is to properly balance the local amphiphilicity of the polymer, *i.e.*, the ratio of cationic to hydrophobic units.⁴²

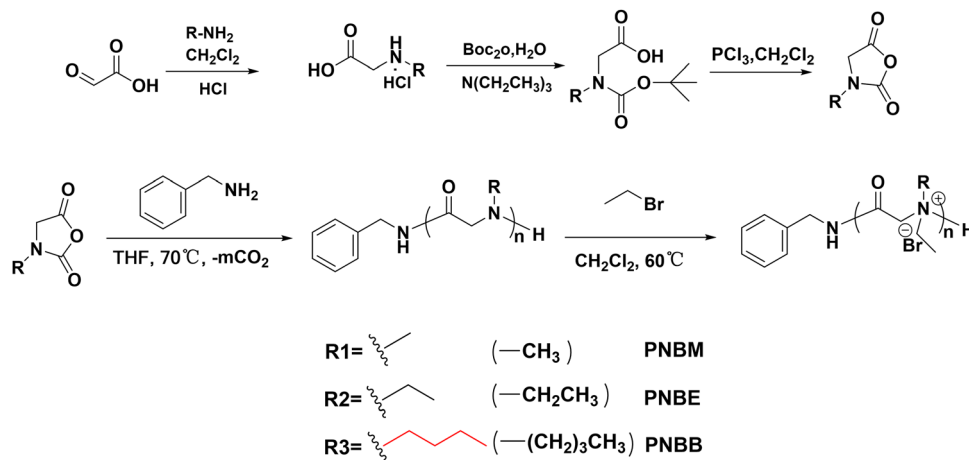
Herein, we prepared a series of cationic polypeptoids by ring-opening polymerization (ROP) and one-step quaternization of the N atom on the main chain. The hydrophobic fragments are regulated by the different side chain carbon lengths and, for this purpose, we designed polypeptoids with different side chain lengths (1C, 2C, 4C) and cationized them under the same conditions. In general, hydrophobic groups, especially lipophilic alkyl groups, are used to enhance antibacterial properties. However, they can also lead to an increase in hemolysis. Conversely, higher hydrophilicity leads to a decrease in toxicity, but also

affects antibacterial activity.⁴³ We systematically investigated the effects of hydrophobic fragments on the antibacterial activity and selectivity. In contrast to previous studies, we found that four carbon-chain-length side chain moieties still did not cause non-negligible cytotoxicity in the highly hydrophobic case. Furthermore, different carbon chain lengths selectively killed *E. coli* and *S. aureus*, which effectively avoids the crisis that inactivation of a specific antibacterial would cause cytotoxicity. Unlike *S. aureus*, *E. coli* has an additional layer of lipopolysaccharide (LPS) in its outer wall, which makes it more difficult to break. Therefore, the “selectivity” is passively caused by the proven mechanism of membrane breaking. The presence of large spatial site resistance in the material structures and the different solubilities of polymers are factors that make it difficult for the polymers to adhere firmly to the material surface to achieve the desired antibacterial effect.^{44,45} After verifying the antibacterial effect and selectivity of the above-mentioned polymers in solution, we introduced PNBB, a polymer with broad-spectrum bactericidal effect, to the surface of polyurethane (PU) substrates. The PU-PNBB films were found to still exhibit contact killing ability against bacteria both *in vivo* and *in vitro*. The enhanced hydrophobicity no longer triggers cytotoxicity of concern and this work provides a solution to address targeted elimination of infections by antimicrobial agents applied to surfaces.

2. Results and discussion

The polypeptoids were first synthesized by ROP using *N*-methyl *N*-carboxyanhydride (Me-NCA), *N*-ethyl *N*-carboxyanhydride (Et-NCA) and *N*-butyl *N*-carboxyanhydride (Bu-NCA) with benzylamine (BnNH₂) as the initiator. This was followed by quaternization with bromoethane to cationize the N atom on the main chain, producing PNBM, PNBE, and PNBB (Scheme 1 and Fig. S1–S6, S10, ESI†). PNBs is the generic umbrella term used for them.

The antibacterial activity of the three quaternized polypeptoids was evaluated by determining their bacteriostatic efficiency against two representative bacteria, Gram-positive bacteria *Staphylococcus aureus* (*S. aureus*) and Gram-negative bacteria *Escherichia coli* (*E. coli*) (Fig. 1a). In all cases, the polymers showed excellent antibacterial performance against Gram-positive bacteria *S. aureus*. We tested the concentration of the polymer corresponding to killing 80% of the bacteria by plate colony counting method (Table 1). Interestingly, PNBM and PNBE were resistant only to Gram-positive bacteria *S. aureus*, due to their positive charge attracting negatively charged bacterial bodies, allowing them to accumulate on the cell wall and creating an inhibiting effect. It is noteworthy that the PNBE sample is more hydrophobic than PNBM, but has a lower ζ -potential than PNBM (Fig. S7 and S8, ESI†). It is conceivable that it is the balance of these two factors that leads to the similar antibacterial activity against *S. aureus*. These results suggest that cationic group action is a key factor in the elimination of Gram-positive pathogens that possess thin cell membranes.



Scheme 1 Synthesis of cationic polypeptides.

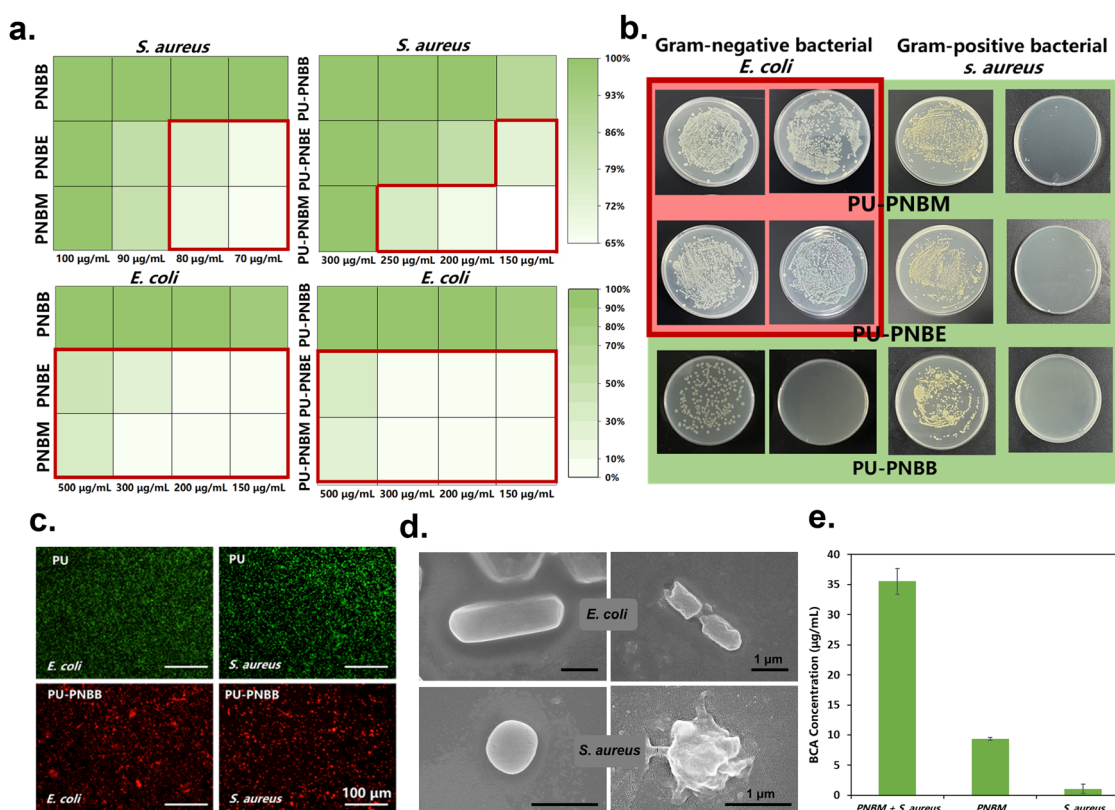


Fig. 1 (a) Bacterial inhibition by PNBs and PU-PNBs against *E. coli* MG1655 and *S. aureus*. In the hot spot plot, a darker color indicates higher inhibition efficiency. (b) Antibacterial selectivity of PU-PNBs (red and green). Colony growth on plate media after co-incubation of PU-PNBs and bacterial solution at a concentration of 300 $\mu\text{g mL}^{-1}$ for 3 h. (c) Live/dead staining assay showing *S. aureus* incubated with PU and PU-PNBs for 3 h. (d) SEM images of film rupture of *E. coli* and *S. aureus*. (e) Leaked protein concentration after co-incubation of PNBB (1 mg mL^{-1}) with *E. coli* (10^7 CFU mL^{-1}) and *S. aureus* (10^5 CFU mL^{-1}). The PBS group was the control group. Data are shown as mean \pm SD ($n = 3$ per group).

It is well known that Gram-negative bacteria *E. coli* displays a double membrane structure with low cell permeability and additional defense mechanisms. Our experiments showed that PNBB had the highest antibacterial activity and increased potential to kill an equivalent amount of *S. aureus* at a concentration of only 80 $\mu\text{g mL}^{-1}$, compared to PNBM and PNBE,

which required 90 $\mu\text{g mL}^{-1}$ to kill 80% of *S. aureus*. In addition, PNBB also exhibited potent antibacterial activity against *E. coli*, independent of the degree of polymerization (DP), killing 80% of *E. coli* at polymer concentrations up to 120 $\mu\text{g mL}^{-1}$. This may be due to the interaction of hydrophobic alkyl chains with hydrophilic groups of bacteria which alters the permeability of

Table 1 Antibacterial activity and hemolytic activity of polymers

Sample	Concentration of 80% antibacterial efficiency ($\mu\text{g mL}^{-1}$)		HC_{10}^a [$\mu\text{g mL}^{-1}$]
	<i>S. aureus</i>	<i>E. coli</i>	
PNBM	90	—	> 2000
PNBE	90	—	> 2000
PNBB	80	120	> 2000
PU-PNBM	260	—	> 2000
PU-PNBE	200	—	> 2000
PU-PNBB	150	150	> 2000

^a The concentration of a polymer that causes 10% hemolysis of hRBC.

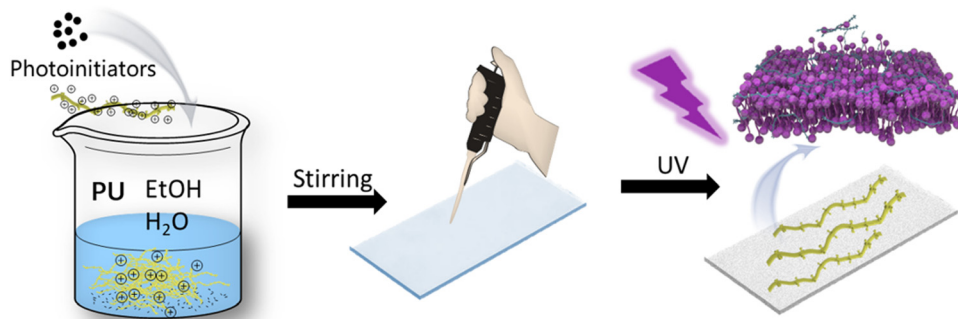
the membrane, disrupting the cell structure and leading to cell lysis and death. Also, the lipopolysaccharide (LPS) in the outer wall of the *E. coli* cell wall enables it to maintain the bacterial structure and even connects them to each other to form biofilms.

Notably, the most hydrophobic PNBB exhibited the lowest ζ -potential of the three, so we suggest that the antibacterial activity shows a non-negligible dependence on the side chain length of the polymer and that this hydrophobic interaction plays a dominant role in killing the Gram-negative bacteria *E. coli*. After clarifying the antibacterial effect of PNBBs in solution, we introduced them onto the surface of a universal glass substrate and prepared PU-PNBBs films (Scheme 2). The plate counting method also showed that PU-PNBBs were able to kill bacteria well at high cell viability concentrations, despite also killing 80% of bacteria at higher concentrations than PNBBs in solution. We have boxed in red the polymer samples with antibacterial efficiency below 80%. It can be seen that both the PNBM and PNBE polymers have only a very low antibacterial effect against *E. coli*, both in the solution proper and on the PU surface (Fig. 1a). Moreover, it was clearly observed on the plate medium that a comparable number of *E. coli* colonies to the control group grew in the experimental groups of PU-PNBM and PU-PNBE when the concentration was $300 \mu\text{g mL}^{-1}$. In contrast, in the experimental group of PU-PNBB, there were almost no clearly visible bacterial colonies on the plates. The difference in hydrophobic fragments still retained this antibacterial selectivity (Fig. 1b). The antibacterial effect of PU-PNBBs was further demonstrated by the results of live/dead fluorescent dyes (Fig. 1c). (Red and green fluorescence represent dead and

surviving bacteria, respectively.) We observed the killing of bacteria after the action of PU-PNBB. This further adds to the proof that this antibacterial effect is independent of the pure PU films on the composite base.

To clarify the antibacterial mechanism of the cationic antimicrobial polypeptoid, we observed obvious cell rupture morphology in SEM images (Fig. 1d). Further, we did BCA (bicinchoninic acid) protein concentration detection experiments. As an example of PNBM solution interacting with *S. aureus*, we added BCA solution to the polymer solution containing the bacteria at 60°C and incubated for half an hour. During this time, divalent copper ions in the solution are reduced to monovalent copper ions by protein under alkaline conditions. The interaction of monovalent copper ions and the unique BCA solution results in a color development reaction. Since the solution shows strong absorbance at 562 nm, the concentration of protein leaking from the bacteria intracellularly was deduced from the good linear relationship between absorbance OD value and protein concentration. The higher the concentration, the more bacteria are ruptured. The control group had no polymer addition. The results are shown in Fig. 1e and Fig. S9 (ESI[†]); the solution with polymer action has significantly more protein, because cations attract the negatively charged bacteria on the surface and the hydrophobic group punctures the bacterial membrane, changing the permeability of the membrane and leading to cell lysis and protein leakage from the interior. We also found that PNBB leaked the most protein and PNBM leaked slightly less than PNBE in the state of co-incubation with the same concentration of polymer and the same colony. This again corroborates that the different abilities of the three polymers to puncture the cell membrane increase with the length of the hydrophobic side chain.

It is generally believed that increasing hydrophobicity improves the ability to lyse RBCs. To investigate the biotoxicity of these antibacterial polypeptoids, we evaluated their hemolysis effect on human red blood cells (hRBCs) using the PNBB samples with the strongest antibacterial effect (most hydrophobic). Notably, despite the presence of four carbon-chain length hydrophobic groups, PNBB exhibited insignificant hemolytic activity (Fig. 2a and Table 1). The insert graph demonstrates the very low hemolysis of the polymer at high concentrations of $1000 \mu\text{g mL}^{-1}$, $900 \mu\text{g mL}^{-1}$, and $800 \mu\text{g mL}^{-1}$, with the supernatant remaining

**Scheme 2** Preparation route of PU-PNBBs film.

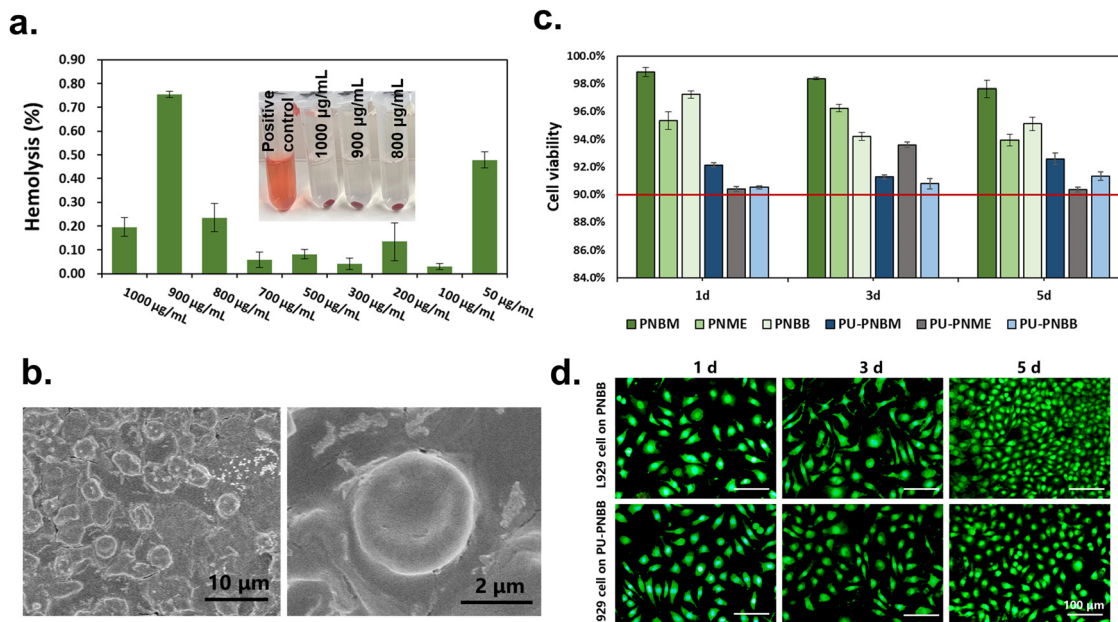


Fig. 2 (a) Hemolysis rate and hemolysis status of PNBB, where the PCR tubes were in the order of positive control, 1000 $\mu\text{g mL}^{-1}$, 900 $\mu\text{g mL}^{-1}$ and 800 $\mu\text{g mL}^{-1}$ sample groups. Data are shown as mean \pm SD ($n = 3$ per group). (b) SEM images of human red blood cells (hRBCs) after being treated with PNBB (1000 $\mu\text{g mL}^{-1}$). Data are shown as mean \pm SD ($n = 3$ per group). (c) Cell viability after incubation with PNBB polymer at a concentration of 1000 $\mu\text{g mL}^{-1}$ for 1, 3 and 5 days against L929 cells. Data are presented as mean \pm standard deviation ($n = 3$). (d) Fluorescence microscope diagram of live/dead stained L929 cells incubated with PNBB and PU-PNBB at a concentration of 1000 $\mu\text{g mL}^{-1}$ for 1, 3 and 5 days.

clear and turbidity-free. (The red clear solution is the positive control.) This is due to the absence of chiral centers in the designed backbone structure and the lack of hydrogen bonding, resulting in generally low hemolysis values of the cationized antibacterial polypeptoids, whether they are in solution or on the glass surface. The SEM images showed that the erythrocytes retained their regular morphology, with an overall round disk shape, slightly depressed in the middle and slightly protruding at the edges, rather than being significantly disrupted (Fig. 2b). The excellent biocompatibility is not diminished with increased antimicrobial effect (increase in hydrophobic side chain length). To further assess the cytotoxicity of PNBBs, we evaluated them by performing a CCK-8 (Cell Counting Kit-8) assay on mouse fibroblastic cells L929. Each PNBB sample exhibited negligible cytotoxicity at a concentration of 80% antibacterial rate and even at 1000 $\mu\text{g mL}^{-1}$ (Fig. 2c). In addition, we observed that the cell survival rate of PU-PNBBs was not as good as that of PNBBs, but the survival rate higher than 90% was considered biocompatible. This decrease may be due to the steric hindrance of the polymeric moieties caused by the introduction of the PU component. Both in the solution proper and on the surface, the number of cells showed a significant proliferation during the cycles of 1, 3 and 5 days of co-incubation of PNBB and PU-PNBB with L929 cells at high concentrations of 1000 $\mu\text{g mL}^{-1}$. The cell morphology was well active and shuttle-shaped, with obvious contours and borders and clearly visible nuclei, and in good growth condition (Fig. 2d). In many studies, the cationic groups and hydrophobic fragments are not in the same center, which greatly increases the difficulty of polymerization.

Biofilm infections are usually associated with chronic infections and are rarely cured. Biofilms exist in structured microbial

communities and are formed by the accumulation of microorganisms and their secretions. The biofilm-producing pathogen *Staphylococcus aureus* has become notorious for chronic infections due to its ability to resist treatment and form biofilms on implanted medical devices, including implanted catheters and joint prostheses.^{46,47} We found that the polypeptoid PNBB had a mechanism of inhibition of bacterial film growth against *S. aureus* after co-incubation of the polymer with bacteria for 48 hours and staining with crystal violet (Fig. 3). The significant decrease in OD value was considered an inhibitory effect of PNBB. This inhibitory effect was also reflected in PU-PNBB. It is obvious from both systems that the inhibitory effect of PU-PNBB film is weaker than that of PNBB solution. We speculate that the introduction of the PU component leads to the steric hindrance of the polymer groups. A portion of the polymer molecules are encapsulated inside the PU film and cannot be released in the biological environment, thus preventing them from contacting the bacteria and killing them.

The antibacterial efficiency of a PU dressing containing polypeptoids for wound anti-infection was evaluated using a *S. aureus* infection model on mouse skin *in vivo*. Using the typical wound infection method, full-thickness wounds were created on the backs of mice using surgical scissors. After 12 hours of *S. aureus* (1×10^7 CFU mL^{-1}) infection, PU-PNBB film dressings were applied to the wound sites (Fig. 4a). No treatment wounds were used as controls. The progression of wound healing showed slow wound healing when wounds were not treated with dressings. In contrast, the PU-PNBB film-covered wounds shrank more rapidly. On day 3, the wound started to crust and healed to only 36% of the original area.

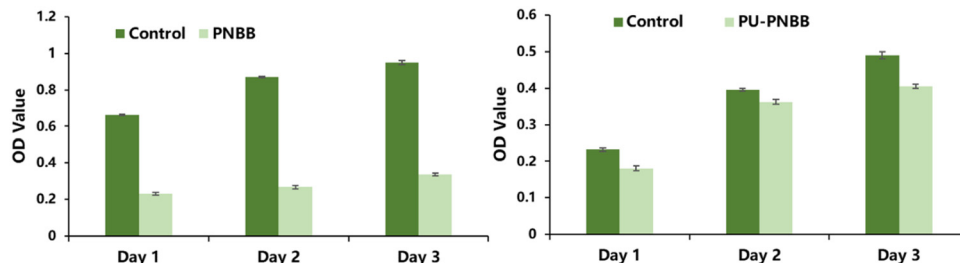


Fig. 3 The OD values of crystalline violet-stained PNBB and PU-PNBB interacting with *S. aureus* biofilm for 24, 48 and 72 h. Data are shown as mean \pm SD ($n = 3$ per group).

Recovery was largely achieved after 7 days of infection (Fig. 4b and c). At the middle of the treatment, six mice from each group had their full-thickness skin around the wound cut off and the bacterial survival rate there was counted by the plate counting method (Fig. 4d and e); it was obvious that the PU-PNBB film-covered wound had less bacteria and even some of the miscellaneous bacteria were effectively killed. The results further demonstrated the excellent *in vivo* antibacterial effect and wound healing potential of the polypeptoids.

3. Conclusions

We have reported a general strategy for the preparation of cationic polypeptoids by ROP and subsequent cationization with a one-step quaternary ammonium method. Polypeptoid PNBBs were introduced to universal glass surfaces together with polyurethane (PU). The antibacterial mechanism of the antibacterial polypeptoids was suggested to be membrane breaking

action leading to cellular cleavage of proteins, which is similar to that of AMP. We attribute this to the fact that the polymers have the same backbone as AMP. We investigated the antibacterial activity and selectivity of PNBBs, considering the importance of the proportion of hydrophobic fragments. A targeted antibacterial effect was achieved by choosing different alkyl chain lengths to modulate the hydrophobic strength. Only four-carbon lengths showed a rapid killing effect against both *S. aureus* and *E. coli*. All materials (PNBBs and PU-PNBBs) showed good biocompatibility which did not deteriorate with the increasing length of the hydrophobic fragments. Good efficiency in inhibiting *S. aureus* biofilm formation was also observed. Among the fabricated materials, PU-PNBB was found to be the most effective, making it a promising candidate for biological applications. In addition, using *S. aureus* infection models on mouse skin, we further showed that the polypeptoids have potent *in vivo* antibacterial efficacy. This simple and efficient cationic polypeptoid formulation with selective antibacterial effect helps provide ideas for achieving therapeutic

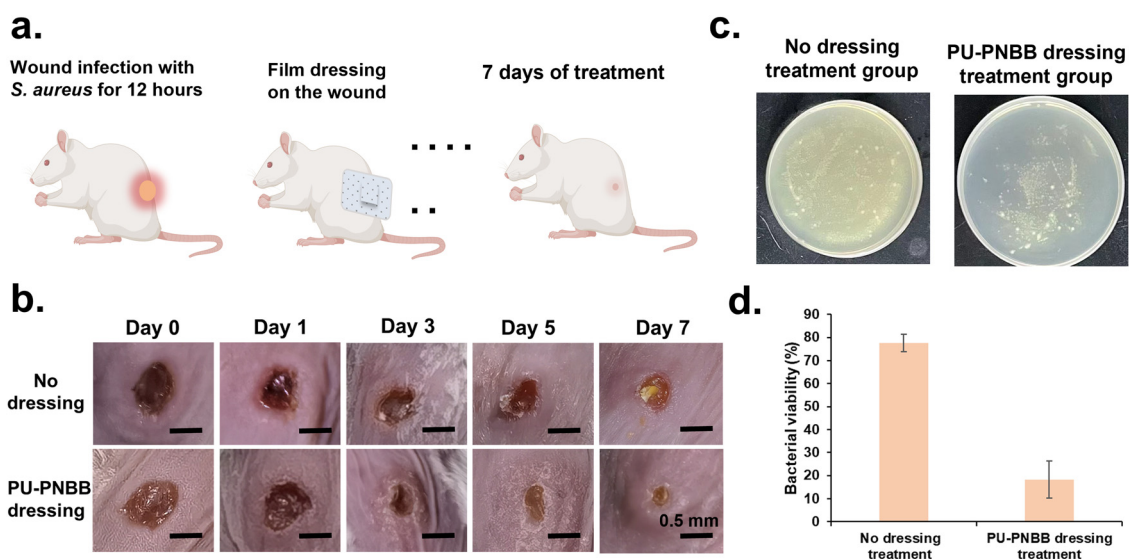


Fig. 4 (a) *In vivo* antibacterial activity of PU-PNBB film dressing against *S. aureus* using a rat full-thickness wound infection model. (b) The digital images of polymer-infected mice skin wounds after being treated with PU-PNBB films at 0, 1, 3, 5, and 7 days. (No dressing treatment was the control group.) (c) Changes in skin wound size in mice treated with PU-PNBB dressing and no dressing. Data are shown as mean \pm SD ($n = 3$ per group). (d) Flat panel image on day 5 after treatment with PU-PNBB dressing. (No dressing treatment was the control group.) (e) Bacterial survival rate on the fifth day after treatment with PU-PNBB dressing (no dressing treatment was the control group.) The plate count method was used. Data are shown as mean \pm SD ($n = 3$ per group).

properties against specific groups of bacteria as well as a viable strategy for introducing antimicrobial agents to the surfaces of biomedical devices.

Conflicts of interest

The authors declare no competing financial interest.

Acknowledgements

We thank the support by Jiangsu Medical Products Administration, Project 1: Research on functional coatings and related technologies for medical devices; Project 2: Research on fastness of the coating of endovascular catheter and guidewire (No. 202013). F. L. thanks Priority Academic Program Development (PAPD) of Jiangsu Higher Education Institutions.

References

- 1 K. A. Brogden, *Nat. Rev. Microbiol.*, 2005, **3**, 238–250.
- 2 M. Zasloff, *Nature*, 2002, **415**, 389–395.
- 3 K. Tang, X. Wang, M. Niu, X. Wang, G. Zhou, J. Shi, Y. Yu, Z. Chen and C. Li, *Adv. Funct. Mater.*, 2022, **32**, 2111344.
- 4 B. P. Lazzaro, M. Zasloff and J. Rolff, *Science*, 2020, **368**, eaau5480.
- 5 G. J. Kelly, A. F.-A. Kia, F. Hassan, S. O'Grady, M. P. Morgan, B. S. Creaven, S. McClean, J. H. Harmey and M. Devocelle, *Org. Biomol. Chem.*, 2016, **14**, 9278–9286.
- 6 R. E. W. Hancock and H.-G. Sahl, *Nat. Biotechnol.*, 2006, **24**, 1551–1557.
- 7 W. Chin, G. Zhong, Q. Pu, C. Yang, W. Lou, P. F. De Sessions, B. Periaswamy, A. Lee, Z. C. Liang, X. Ding, S. Gao, C. W. Chu, S. Bianco, C. Bao, Y. W. Tong, W. Fan, M. Wu, J. L. Hedrick and Y. Y. Yang, *Nat. Commun.*, 2018, **9**, 917.
- 8 M. Zhou, Y. Qian, J. Xie, W. Zhang, W. Jiang, X. Xiao, S. Chen, C. Dai, Z. Cong, Z. Ji, N. Shao, L. Liu, Y. Wu and R. Liu, *Angew. Chem., Int. Ed.*, 2020, **59**, 6412–6419.
- 9 J. Xie, M. Zhou, Y. Qian, Z. Cong, S. Chen, W. Zhang, W. Jiang, C. Dai, N. Shao, Z. Ji, J. Zou, X. Xiao, L. Liu, M. Chen, J. Li and R. Liu, *Nat. Commun.*, 2021, **12**, 5898.
- 10 M. Shepida, O. Kuntiyi, Y. Sukhatskiy, A. Mazur and M. Sozanskyi, *Bioinorg. Chem. Appl.*, 2021, **2021**, 4465363.
- 11 M. F. Ilker, K. Nüsslein, G. N. Tew and E. B. Coughlin, *J. Am. Chem. Soc.*, 2004, **126**, 15870–15875.
- 12 X. Wang, F. Yang, H. Yang, X. Zhang, H. Tang and S. Luan, *Biomater. Sci.*, 2022, **10**, 834–845.
- 13 M. Xiong, M. W. Lee, R. A. Mansbach, Z. Song, Y. Bao, R. M. Peek, C. Yao, L.-F. Chen, A. L. Ferguson, G. C. L. Wong and J. Cheng, *Proc. Natl. Acad. Sci. U. S. A.*, 2015, **112**, 13155–13160.
- 14 Y. Shi, P. Teng, P. Sang, F. She, L. Wei and J. Cai, *Acc. Chem. Res.*, 2016, **49**, 428–441.
- 15 C. Ghosh, P. Sarkar, S. Samaddar, D. S. S. M. Uppu and J. Haldar, *Chem. Commun.*, 2017, **53**, 8427–8430.
- 16 Y. Liu, S. Ding, R. Dietrich, E. Märtilbauer and K. Zhu, *Angew. Chem., Int. Ed.*, 2017, **56**, 1486–1490.
- 17 Y. Niu, M. Wang, Y. Cao, A. Nimmagadda, J. Hu, Y. Wu, J. Cai and X.-S. Ye, *J. Med. Chem.*, 2018, **61**, 2865–2874.
- 18 H. C. Schunk, M. J. Austin, B. Z. Taha, M. S. McClellan, L. J. Suggs and A. M. Rosales, *Mol. Syst. Des. Eng.*, 2023, **8**, 92–104.
- 19 D. Zhang, S. H. Lahasky, L. Guo, C.-U. Lee and M. Lavan, *Macromolecules*, 2012, **45**, 5833–5841.
- 20 J. Tian, J. Sun and Z. Li, *Polymer*, 2018, **138**, 132–138.
- 21 B. S. Tucker, S. G. Getchell, M. R. Hill and B. S. Sumerlin, *Polym. Chem.*, 2015, **6**, 4258–4263.
- 22 M. Barz, R. Luxenhofer, R. Zentel and M. J. Vicent, *Polym. Chem.*, 2011, **2**, 1900–1918.
- 23 K. Kirshenbaum, A. E. Barron, R. A. Goldsmith, P. Armand, E. K. Bradley, K. T. V. Truong, K. A. Dill, F. E. Cohen and R. N. Zuckermann, *Proc. Natl. Acad. Sci. U. S. A.*, 1998, **95**, 4303–4308.
- 24 A. E. Barron and R. N. Zuckerman, *Curr. Opin. Chem. Biol.*, 1999, **3**, 681–687.
- 25 K. Kirshenbaum, R. Zuckermann and K. Dill, *Curr. Opin. Struct. Biol.*, 1999, **9**, 530–535.
- 26 L. Guo, J. Li, Z. Brown, K. Ghale and D. Zhang, *Biopolymers*, 2011, **96**, 596–603.
- 27 Z. S. Clauss and J. R. Kramer, *ACS Appl. Mater. Interfaces*, 2022, **14**, 22781–22789.
- 28 B. L. Bray, *Nat. Rev. Drug Discovery*, 2003, **2**, 587–593.
- 29 M. Sieprawska-Lupa, P. Mydel, K. Krawczyk, K. Wójcik, M. Puklo, B. Lupa, P. Suder, J. Silberring, M. Reed, J. Pohl, W. Shafer, F. McAleese, T. Foster, J. Travis and J. Potempa, *Antimicrob. Agents Chemother.*, 2004, **48**, 4673–4679.
- 30 C. Zhou, X. Qi, P. Li, W. N. Chen, L. Mouad, M. W. Chang, S. S. J. Leong and M. B. Chan-Park, *Biomacromolecules*, 2010, **11**, 60–67.
- 31 A. C. Engler, A. Shukla, S. Puranam, H. G. Buss, N. Jreige and P. T. Hammond, *Biomacromolecules*, 2011, **12**, 1666–1674.
- 32 Q. Gao, P. Li, H. Zhao, Y. Chen, L. Jiang and P. X. Ma, *Polym. Chem.*, 2017, **8**, 6386–6397.
- 33 A. Sulistio, A. Blencowe, A. Widjaya, X. Zhang and G. Qiao, *Polym. Chem.*, 2012, **3**, 224–234.
- 34 A. Sulistio, A. Widjaya, A. Blencowe, X. Zhang and G. Qiao, *Chem. Commun.*, 2011, **47**, 1151–1153.
- 35 L. Yu, K. Li, J. Zhang, H. Jin, A. Saleem, Q. Song, Q. Jia and P. Li, *ACS Appl. Bio Mater.*, 2022, **5**, 366–393.
- 36 V. Sambhy, B. R. Peterson and A. Sen, *Angew. Chem., Int. Ed.*, 2008, **47**, 1250–1254.
- 37 P. Pham, S. Oliver, D. T. Nguyen and C. Boyer, *Macromol. Rapid Commun.*, 2022, **43**, 2200377.
- 38 H. Mortazavian, L. L. Foster, R. Bhat, S. Patel and K. Kuroda, *Biomacromolecules*, 2018, **19**, 4370–4378.
- 39 C. Secker, J. W. Robinson and H. Schlaad, *Eur. Polym. J.*, 2015, **62**, 394–399.
- 40 J. Sun, M. Li, M. Lin, B. Zhang and X. Chen, *Adv. Mater.*, 2021, **33**, 2104402.
- 41 Z. Lu, Y. Wu, Z. Cong, Y. Qian, X. Wu, N. Shao, Z. Qiao, H. Zhang, Y. She, K. Chen, H. Xiang, B. Sun, Q. Yu, Y. Yuan, H. Lin, M. Zhu and R. Liu, *Bioact. Mater.*, 2021, **6**, 4531–4541.
- 42 R. Liu, X. Chen, S. Chakraborty, J. J. Lemke, Z. Hayouka, C. Chow, R. A. Welch, B. Weisblum, K. S. Masters and S. H. Gellman, *J. Am. Chem. Soc.*, 2014, **136**, 4410–4418.

- 43 M. A. Rahman, M. Bam, E. Luat, M. S. Jui, M. S. Ganewatta, T. Shokfai, M. Nagarkatti, A. W. Decho and C. Tang, *Nat. Commun.*, 2018, **9**, 5231.
- 44 C. D. Nadell, K. Drescher and K. R. Foster, *Nat. Rev. Microbiol.*, 2016, **14**, 589–600.
- 45 M. Henze, D. Mädge, O. Prucker and J. Rühle, *Macromolecules*, 2014, **47**, 2929–2937.
- 46 J. Baishya and C. A. Wakeman, *npj Biofilms Microbiomes*, 2019, **5**, 16.
- 47 D. E. Moormeier and K. W. Bayles, *Mol. Microbiol.*, 2017, **104**, 365–376.